

UC Berkeley

UC Berkeley Previously Published Works

Title

Approaching 100% Selectivity at Low Potential on Ag for Electrochemical CO₂ Reduction to CO Using a Surface Additive

Permalink

<https://escholarship.org/uc/item/82v03622>

Journal

ACS Catalysis, 11(15)

ISSN

2155-5435

Authors

Buckley, Aya K
Cheng, Tao
Oh, Myoung Hwan
[et al.](#)

Publication Date

2021-08-06

DOI

10.1021/acscatal.1c00830

Peer reviewed

Approaching 100% Selectivity at Low Potential on Ag for Electrochemical CO₂ Reduction to CO Using a Surface Additive

Aya K. Buckley,^{1,2,3,‡} Tao Cheng,^{4,5,‡} Myoung Hwan Oh,¹ Gregory M. Su,^{6,7} Jennifer Garrison,^{1,2,3} Sean W. Utan,^{1,2,3} Chenhui Zhu,⁶ F. Dean Toste,^{1,2,3,} William A. Goddard III,^{5,*} Francesca M. Toma^{1,2,*}.*

¹Joint Center for Artificial Photosynthesis, Lawrence Berkeley National Laboratory, 1 Cyclotron Road, Berkeley, CA 94720, USA.

²Chemical Sciences Division, Lawrence Berkeley National Laboratory, 1 Cyclotron Road, Berkeley, CA 94720, USA.

³Department of Chemistry, University of California, Berkeley, CA 94720, USA

⁴Institute of Functional Nano & Soft Materials (FUNSOM), Jiangsu Key Laboratory for Carbon-Based Functional Materials & Devices, Joint International Research Laboratory of Carbon-Based Functional Materials and Devices, Soochow University, 199 Renai Road, Suzhou, 215123, Jiangsu, PR China

⁵Joint Center for Artificial Photosynthesis and Materials and Process Simulation Center; California Institute of Technology, Pasadena CA, 91125, USA

⁶Advanced Light Source, Lawrence Berkeley National Laboratory, 1 Cyclotron Road, Berkeley, CA 94720, USA

⁷Material Sciences Division, Lawrence Berkeley National Laboratory, 1 Cyclotron Road, Berkeley, CA 94720, USA

KEYWORDS

electrochemical CO₂ reduction, surface additives, interfaces, silver, molecular dynamics

ABSTRACT

We report the discovery of a quaternary ammonium surface additive for CO₂ reduction on Ag surfaces that changes the Faradaic efficiency for CO from 25% on Ag foil to 97%, while increasing the current density for CO production from 0.14 to 1.2 mA/cm². Using ReaxFF reactive molecular dynamics, we find that the surface additive with the highest selectivity, dihexadecyldimethylammonium bromide, promotes substantial population of CO₂ near the Ag surface along with sufficient H₂O to activate the CO₂. While a critical number of water molecules is required in the CO₂ reduction to CO, the trend in selectivity strongly correlates with the availability of CO₂ molecules. We demonstrate that the ordering of the cationic modifiers plays a significant role around the active site, thus determining reaction selectivity. The dramatic improvement by addition of a simple surface additive suggests a new strategy in electrocatalysis.

INTRODUCTION

The complexity of the Electrode-Electrolyte Interface (EEI) clouds the rational design of electrocatalysts that promote the selective formation of specific products in

electrocatalytic reactions.¹ Efforts to tune a single parameter, such as the electrolyte, can have a wide-ranging influence on many related features, including the local pH, electric field, or binding of surface species.² As a result, tuning the selectivity of reactions, such as the reduction of CO₂, by varying one component often raises additional questions regarding the mechanism underlying the observed change in catalytic behavior.

Organic species have been employed to tune the CO₂ reduction behavior of metallic catalysts.³⁻⁴ However, the mechanism for the observed changes in selectivity in these systems remains uncertain. For example, Masel *et al.* reported that the ionic liquid 1-ethyl-3-methylimidazolium tetrafluoroborate lowered the overpotential for the formation of CO from CO₂ on Ag surfaces.⁵ A number of mechanisms for the changes observed in the presence of this and other organic modifiers have been proposed in the literature and examined via variations to the organic structure,⁶ spectroscopic methods⁷⁻⁸ or theoretical studies.⁹ These hypotheses include the suppression of the competing hydrogen evolution reaction (HER),¹⁰ interaction with CO₂⁻ radical or other possible

intermediates in solution¹¹ or at the metal surface,¹² and tuning of the reaction microenvironment.¹³ These numerous suggested mechanisms indicate that multiple parameters may exert an influence on the catalytic system and a consensus has yet to emerge as to which has the most substantial impact on the reaction outcome.

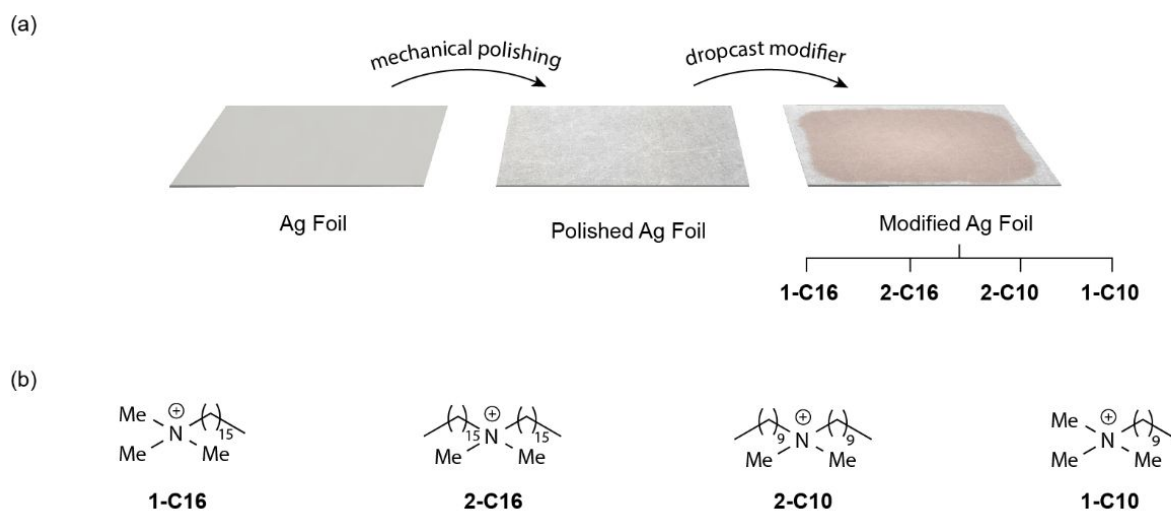
We recently considered these challenges in the context of CO₂ reduction on Cu at a low potential, where we identified the most sensitive and influential selectivity-determining factors, rather than through the study of a single chosen parameter.¹⁴ By examining the effect of a diverse but structurally simple set of organic species on product selectivity, we identified the characteristics that played the most influential role in dictating the observed selectivity. On Cu surfaces, the hydrophilicity/phobicity of the organic modifiers emerged as a notable feature that dictated whether formic acid or CO was favored. Within the series of hydrophobic organic modifiers that were examined, a cationic functionality was found to be important for improved selectivity for CO, an observation that remained unexplained.

To examine specifically the role of the cation in CO formation, we applied cationic modifiers from our previous studies on Cu to the reduction of CO₂ to CO formation on Ag at low potential. We find that a particular alkylammonium cation leads to 97% Faradaic efficiency (FE) for reduction of CO₂ to CO while increasing the current by a factor of ~8.6. To understand the origins of this dramatic improvement in performance, we carried out reactive molecular dynamics simulations using the ReaxFF reactive force field. We find that the selectivity of each cationic modifier is related to the surface concentration of CO₂ maintained on the modified Ag surface. While the presence of a critical number of water molecules at the catalytic site is necessary because water participates in the formation of a key intermediate (HOCO*) in the mechanism of CO₂ reduction to CO, ensuring a high availability of CO₂ is of primary importance in CO production. We demonstrate that the availability of both CO₂ and H₂O around the active site markedly depends on the ordering of cationic modifiers.

These results are significant for gas diffusion electrode configurations, where

interactions of the catalyst with ionomers and polymers can have an impact on tuning

the reaction selectivity. Additionally, these findings contribute to providing a complete picture of the selectivity-determining factors in CO₂ reduction, thus suggesting new strategies to develop architectures in tandem catalytic processes to produce very selective organic products. More generally, these results highlight the utility of identifying the most sensitive and tunable parameters in a given system as a paradigm for the design of organic species that promote a specific product.



Scheme 1. Fabrication of modified Ag surfaces with quaternary ammonium salts. (a)

Schematic representation of the modification of the Ag electrode with different cationic modifiers. (b) Structure of cationic modifiers used in this study:

hexadecyltrimethylammonium bromide (**1-C16**), dihexadecyldimethylammonium

bromide (**2-C16**), didecyldimethylammonium bromide (**2-C10**), and trimethyldecylammonium bromide (**1-C10**).

RESULTS AND DISCUSSION

To shed light on how to influence CO formation on Ag, we focused on the catalytic behavior at the onset of CO formation by examining the CO₂ reduction behavior at low potential (-0.8 V vs. RHE). Therefore, CO₂ reduction selectivity of Ag foil and Ag, in the presence of a series of quaternary alkylammonium salts, were characterized to determine which features of the ammonium salts are key to influencing CO formation. Briefly, the modified Ag surfaces were prepared by mechanical polishing of Ag foil. A solution of the quaternary alkylammonium salt under investigation was then drop-cast onto the Ag polished surface (Scheme 1a). The cationic modifiers are characterized by the presence of two or three methyl substituents to the N atom with two or one longer carbon chains. For the sake of clarity, we highlight this feature with a nomenclature

specifying the number and length of the alkyl chain as substituents to the N atom

(Scheme 1b).

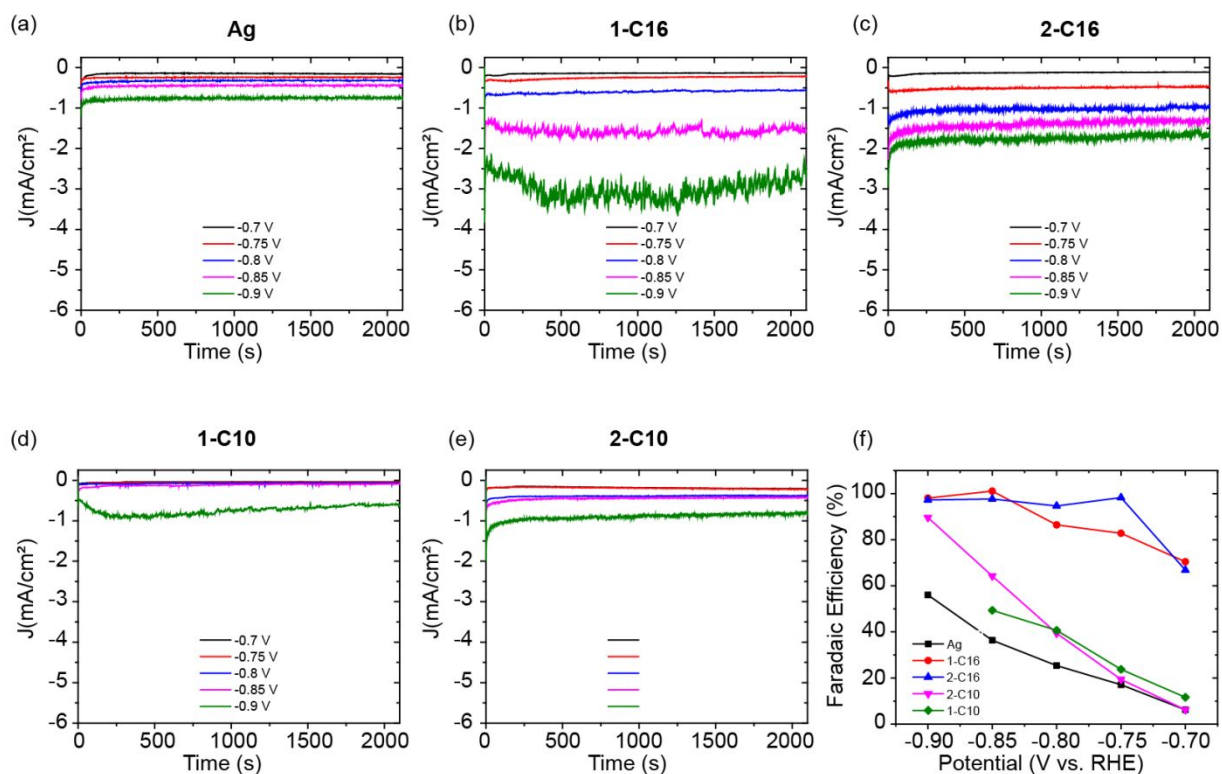


Figure 1. Chronoamperometry of (a) Ag, and functionalized (b) 1-C16, (c) 2-C16, (d) 1-C10, (e) 2-C10 Ag samples at different potentials for 35 minutes, as well as Faradaic Efficiency of the different samples at different potentials.

The behavior of the Ag foil modified with quaternary ammonium salts of varying substitution patterns was analyzed in order to establish the influence of these salts on the product distribution (Figure 1). The testing procedure involved placement of polycrystalline Ag foil in a cell of previously reported design,¹⁵ and evaluation of the CO₂ reduction behavior over a time period of 35 minutes. Related chronoamperometries have a stable trend over the time of the experiment (Figure 1). In order to verify that these cationic modifiers maintain their chemical structure throughout the experiment, the electrodes were rinsed after the chronoamperometric experiments and the structures of the organic modifiers obtained from this washing were characterized using NMR (Supporting Information, Figure S1-S8). The resulting spectra indicated that the cationic modifiers remain intact in the presence of the applied potential. The analysis of the selectivity of the modifiers shows that trimethyldecylammonium bromide **1-C10** and didecyldimethylammonium bromide (**2-C10**) have similar selectivity for CO across different potentials, ranging from -0.7 V to -0.9 V vs. RHE. On the other hand, while hexadecyltrimethylammonium bromide (**1-C16**) and dihexadecyldimethylammonium

bromide (**2-C16**) exhibit similar behavior at -0.7 V and -0.9 V vs RHE, **2-C16**

approaches ~100% FE for CO already at -0.75 V vs RHE.

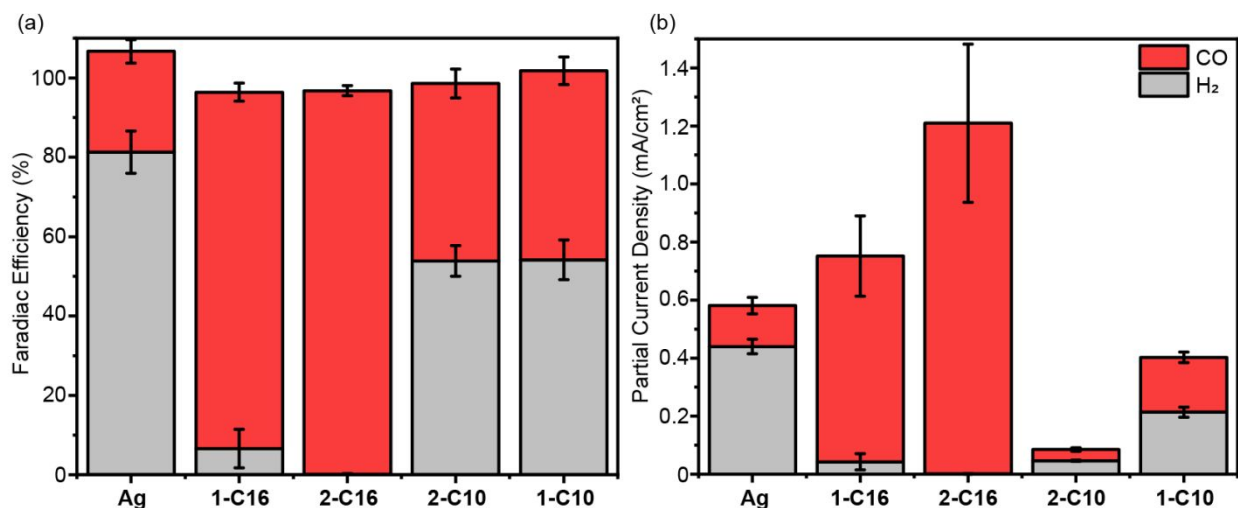


Figure 2. (a) Dramatically increased selectivity for CO is observed with modifiers **1-C16** and **2-C16** compared to CO formation using **2-C10** and **1-C10**. Values and error bars are calculated from three trials, with error bars reported as standard error of the mean (SEM).

(b) Partial current densities of functionalized Ag surfaces and Ag foil at -0.8 V vs. RHE.

2-C16 leads to ~8 times increased activity towards CO with significantly decreased activity for H₂. Values are expressed as geometric current densities. Product distribution data was determined via chronoamperometry experiments conducted for 35 minutes.

Values are averages of three trials, with error bars reported as standard error of the mean.

Therefore, to understand the reasons for discrete difference in selectivity, we focused at -0.8 V (Figure 2), where chronoamperometry traces show high stability and difference in selectivity among different modifiers are more pronounced. The resulting product distribution were measured as a function of Faradaic efficiency (FE%), and for Ag foil closely resembled previous reports for polycrystalline Ag.¹⁶ In similar experiments carried out on Cu, we had previously observed that the relatively hydrophilic **1-C16** and **2-C10** promoted H₂ and formic acid formation via weakening of the metal-hydride interaction in the hydrophilic environment. In contrast, hydrophobic **2-C16** promoted CO formation under otherwise identical conditions. On the basis of the experiments on Cu, we posited that CO₂R on Ag would also generate more H₂ when modified with **1-C16** and **2-C10**, and more CO with **2-C16**. Indeed, we found Ag surfaces modified with **2-C16** demonstrate an extremely high FE of 97% at -0.8 V vs. RHE, while Ag surfaces modified with **1-C16** show lower FE of 90% for CO at -0.8 V. Moreover, the experiment using Ag with modifier **2-C10** found that the reaction was only slightly more selective for

CO than the unfunctionalized surface, with FE of 45%. Intrigued by this behavior, the effect of **1-C10** was also examined and showed a selectivity (FE 48%) similar to Ag surfaces modified with 2-C10. The observed trend marks an enhancement in CO selectivity specific to ammonium salts with long, 16-carbon chains.

The partial current densities show that the amount of CO formed by unfunctionalized Ag surfaces increases by a factor of ~ 8.6 from 0.14 to 1.21 mA/cm², while the amount of H₂ is almost completely suppressed to 0.001 mA/cm² in the presence of **2-C16** (Figure 2b).

As a result, these observations indicate that the changes in selectivity could result from mechanistic variations that either facilitate CO formation, suppress H₂ formation or some combination of both.

The trend related to hydrocarbon chain length provides interesting clues into which features of these ammonium salts are important to influencing catalysis at the Ag surface. In our previous studies on Cu, we found that whether the ammonium salt was di- or trimethyl substituted and the lengths of the hydrocarbon chains both impacted the hydrophilicity/phobicity of the surface and the selectivity of the reaction.

Hydrophilicity measurements of the functionalized Ag surfaces were characterized with a goniometer (Supplemental Information, Table S1). In this Ag system, similar hydrophilicities were observed for **1-C16**, **2-C10**, and **1-C10**. The surface tension of the liquid/solid interfaces predicted from molecular dynamic simulations are consistent with the measured contact angles. However, **1-C16** and **2-C16** showed high selectivity for CO formation, whereas selectivity for CO was reduced with **2-C10** and **1-C10** as modifiers, indicating that the hydrophilicity is not the dominant factor determining the selectivity.

The presence of surrounding water has been implicated in mechanisms for CO formation on Ag.¹⁷⁻¹⁸ However, there is a lack of direct correlation between CO selectivity and hydrophilicity/phobicity of the modifier on Ag differs from Cu.¹⁴

Specifically, in the selective conversion of CO₂ to CO on Ag surfaces, the selectivity-determining change is *not* dominated by the interaction of these cationic species with the surrounding water. We ascribe this different behavior to the presence of multiple CO₂ reduction mechanisms involving protons on the Cu surface. The formation of both

HCOOH and CO involves several protons and needs the presence of a proton source (H₂O). In the selective conversion of CO₂ to CO on the Ag surface at low potential the presence of a proton source, yet important, appears less critical. In addition, the series in Figure 2 suggests that the presence of a cationic functionality or bromide anion is *not* sufficient to observe a significant enhancement in CO selectivity. On the other hand, the change from C10 to C16 substituents has a marked impact on the influence of these ammonium salts on product selectivity. Moreover, previous studies suggest that the length of these alkyl chains plays an important role in the ordering of these molecules. For example, Osman reported that a self-assembled monolayer of ammonium salts undergoes a change in conformation upon heating, with a more pronounced reliance on chain length than on the number of long hydrocarbon substituents.¹⁹ Nevertheless, we observe that the number of hydrocarbon chains, in a fixed length, adjusts the hydrophilicity that seems to fine-tune the CO selectivity. Consequently, we sought to understand the behavioral changes that might arise with this dependence on chain length and the number of long hydrocarbon chains or overall hydrocarbon content, such as the ordering of cationic modifiers.

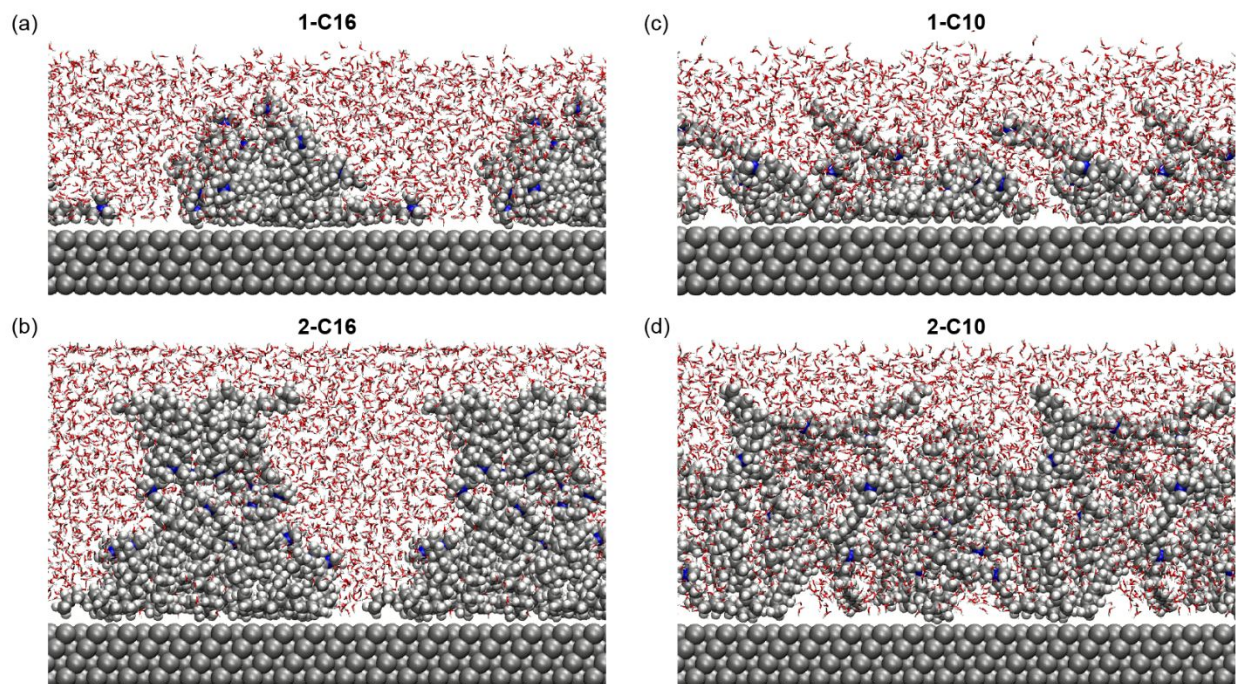


Figure 3. The last snapshot of the interface between Ag, water, CO₂ and **1-C16** (a), **2-C16** (b), **1-C10** (c), **2-C10** (d), extracted from 2 ns of RMD canonical ensemble (NVT) simulations at 298 K to equilibrate the interface. The width of the picture is 9.20 nm and the height is 5 nm. The colors are N in blue, C in gray, O in red, and H in white.

In order to further understand the interaction of these ammonium salts with each other, the surrounding water, CO₂, and the Ag surface, we carried out Reactive Molecular Dynamics (RMD) simulations using the ReaxFF reactive force field for all four salts.²⁰

The simulation models were built following the same procedure as reported previously, but with the force field parameters changed from Cu to Ag.¹⁴ We tested the neutral case with 26 Br⁻ (Figure 3) and the cases with 24 and 25 ions, where we find similar results (Figure S9). The simulation results show that the distribution of both cations and anions are almost the same. This change decreases slightly the interaction of the metal with the interfacial water and ammonium salts. We carried out 2 ns RMD simulations to equilibrate the interface, which we previously demonstrated to be sufficient equilibration time. Snapshots of the predicted interface structure are shown in Fig. 2.

An examination of ammonium salts in the simulations indicates that the changes in structure between the four modifiers are accompanied by changes in segregation of CO₂ and H₂O at the interface. We observe that modifier **2-C16** forms a bilayer at the interface, with the ammonium groups facing inward between the two layers. Modifier **1-C16** forms a monolayer at the interface, with the hydrocarbon chains aggregated at the Ag surface with the ammonium groups facing outward towards the surrounding water. Modifiers **2-C10** and **1-C10** show less phase segregation, with the water better

intercalated with the cationic species. The differences in catalytic behavior between the systems with C16 and C10 substituted ammonium salts can be due to conformational differences at the electrode interface. While three of these four modifiers demonstrate a similar hydrophilicity, the longer hydrocarbon chains in **1-C16** and **2-C16**, allow these two molecules to form an organized layer that changes the interfacial environment.

Although the interfacial environment is known to have a substantial impact on the product selectivity in the CO₂ reduction reaction,^{13, 21} the ordering of organic modifiers, including ionic liquid-type promoters, is relatively underexplored. In one example, the Dlott group examined the conformation of imidazolium salts on Ag using sum frequency generation spectroscopy.⁴ They found that the salts undergo a structural transition at potentials similar to the onset of CO formation and suggested that the ordering of the salts may play an important role in their ability to promote CO selectivity. Therefore, we hypothesize that we are observing a similar phenomenon with a structurally distinct set of organic compounds.

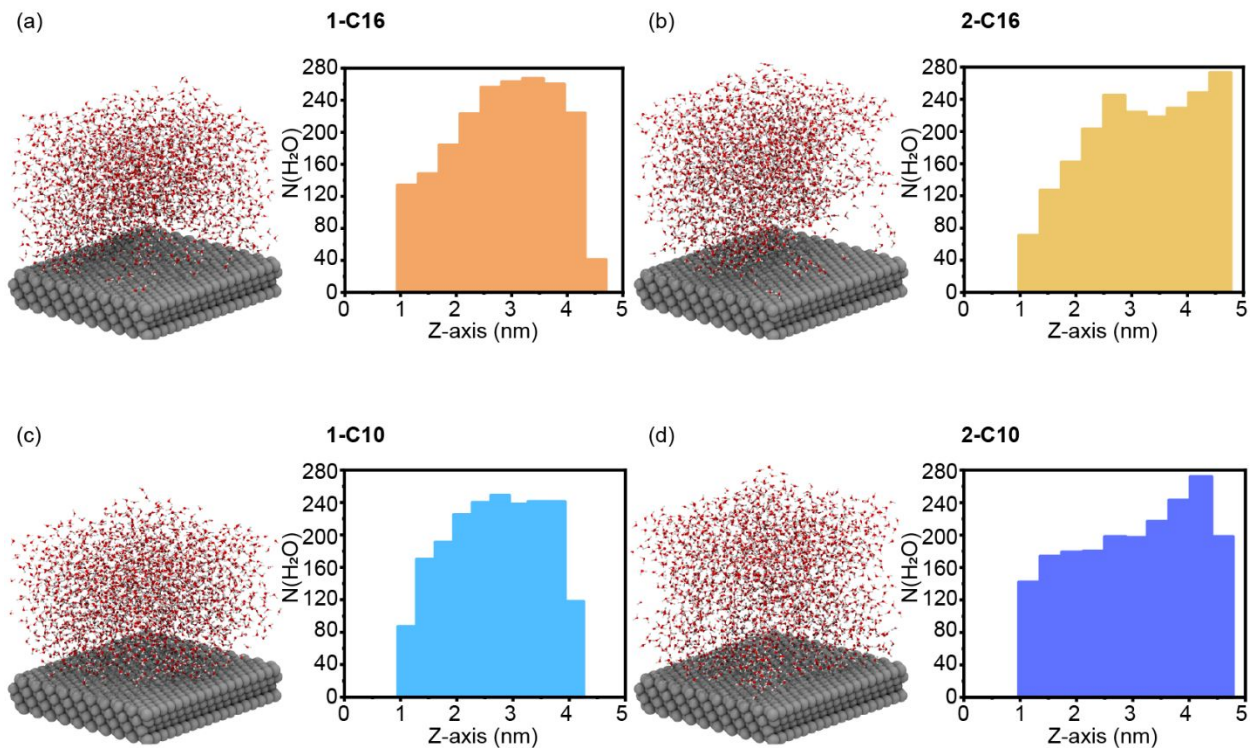


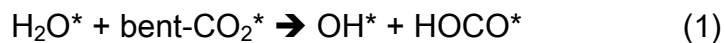
Figure 4. Different snapshots were obtained by removing the cationic modifier and CO_2 molecules. The snapshots and histograms of water molecules' distribution at the Ag surface and as a function of the distance from the surface (Z-axis), respectively, are reported for **1-C16** (a), **2-C16** (b), **1-C10** (c), **2-C10** (d).

We then turned to the question of how this difference in ordering affects the catalytic behavior at the Ag surface. Figure 4 shows the distribution of water molecules at the

modified Ag surface. The **2-C16** modified surface is the most hydrophobic, and has the least amount of water molecules at the interface. Conversely, **1-C16** shows similar or more water molecules near the interface than the organic modifiers with 10-carbon chains, which suggests that the availability of H₂O is substantially dependent on the ordering of the cationic modifiers rather than strictly reliant on the hydrocarbon chain length.

To examine the distribution of sites that favor CO₂ binding with $\Delta E < 0$, the possible CO₂ solvation sites were estimated by employing the test particle insertion method by Widom to calculate the distribution of CO₂ in regions close to the interface after ReaxFF MD simulation.²²

From our previous studies of the mechanism of CO₂ reduction to CO, we know that the critical intermediate is formation of the HOCO* intermediate which forms by



Thus, both CO₂ and water must be close to the surface (1).¹⁸ Indeed Figure 5 shows that **2-C16** has 45 CO₂ in the first monolayer (ML) compared to 27 for **1-C16**, 18 for **2-C10**, and 14 for **1-C10** (see Supporting Information). Moreover **2-C16** retains 111 CO₂ near the surface (≤ 4 nm) compared to 81 for **1-C16**, 33 for **2-C10**, and 30 for **1-C10** (Table 1). Some H₂O at the interface for CO₂R is also required, but not so much as to promote HER. Again **2-C16** seems best in this regard. Interestingly, the distribution of water and CO₂ molecules has been analyzed also for the bare Ag surface, where there are only 22 CO₂ binding sites (Figure S10).

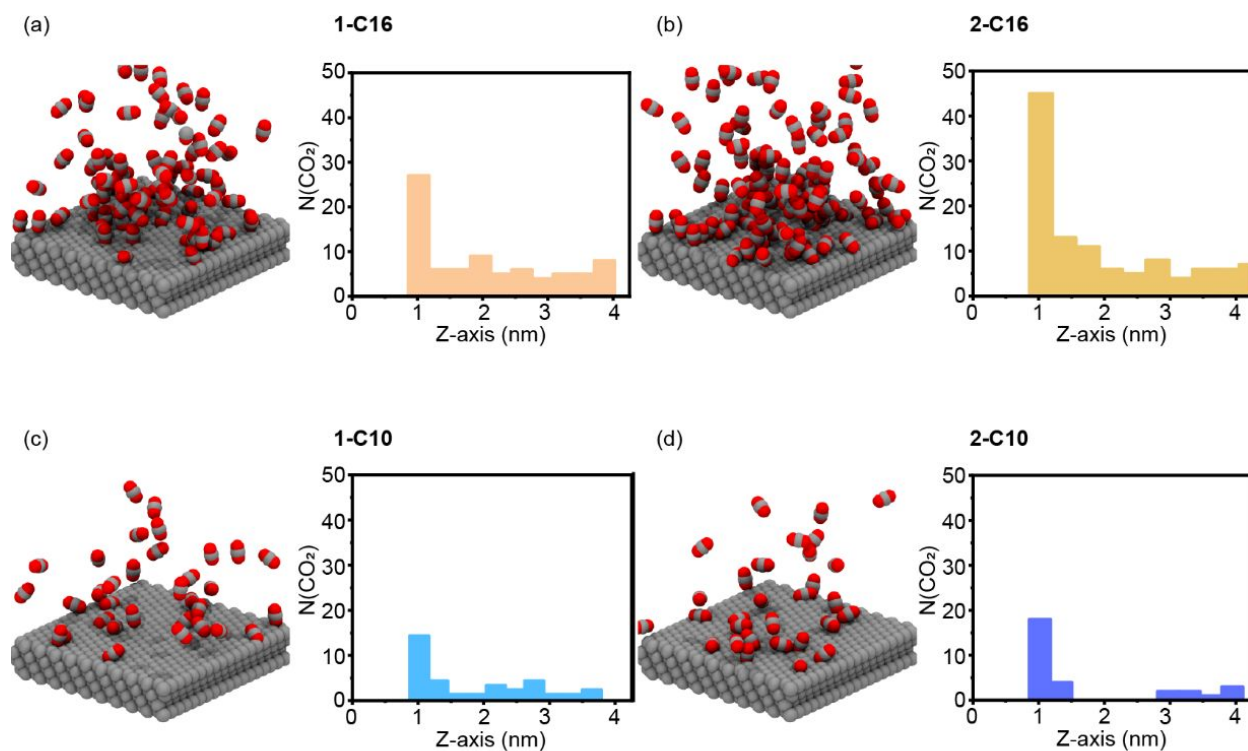


Figure 5. Different snapshots were obtained by removing the cationic modifier and water molecules. The snapshots and histograms of CO₂ molecules' distribution at the Ag surface and as a function of the distance from the surface (Z-axis), respectively, are reported for **1-C16** (a), **2-C16** (b), **1-C10** (c), **2-C10** (d).

This analysis of the CO₂ distribution highlights that **2-C16** demonstrates higher CO selectivity (FE = 97%) and has a higher concentration of CO₂ at the Ag surface.

Interestingly, **1-C16** also shows a high number of CO₂ molecules in proximity of the Ag surface, accompanied by high CO selectivity (FE = 90%). On the other hand, **1-C10** and **2-C10** both show a decreased number of CO₂ sites, which is in agreement with their lower selectivity (FE = 48% and 45%, respectively) for CO production (Table 1). Thus, the balance between CO₂ availability within a nanometer of the metal surface and the presence of some water molecules provides a mechanistic hypothesis that is consistent with the observed catalytic behavior. To more specifically address this point, we have calculated the coordination number (CN) of CO₂ itself and CO₂ with water. Taking a cutoff of 0.4 nm, the CN of CO₂ to CO₂ is 0.785, and the CN of CO₂ to water is 4.727. Therefore, the ratio of water/CO₂ around CO₂ is about 5, which indicates that at this concentration there is enough water around to provide the proton for the CO₂ reduction reaction (Figure S11). This analysis suggests that the increased local CO₂ concentration enhances the CO₂ reduction reaction over the reduction of protons, with enough local water present for CO formation to proceed.²⁴

Table 1. Relationship between cationic modifier, presence of CO₂, and FE for CO

Cationic Modifier	Sites for CO ₂ binding	FE for CO (%)
Ag	22	25
1-C16	81	90
2-C16	111	97
1-C10	33	48
2-C10	30	45

The investigation of the trans-gauche distributions of the carbon chains in the cationic modifiers also provide more insights into understanding the increased solubility of CO₂ in the **2-C16** case (Figure S12). These results show clearly that **2-C16** has a much higher ratio of gauche configurations with respect to the other cationic modifiers under investigation. This finding suggests that the looser cluster associated with gauche conformations may help accommodate the CO₂, explaining the increased availability. This observation is in agreement with existing literature on polymer packing showing

that the presence of a more rigid structure may negatively influence diffusion of molecules.²³

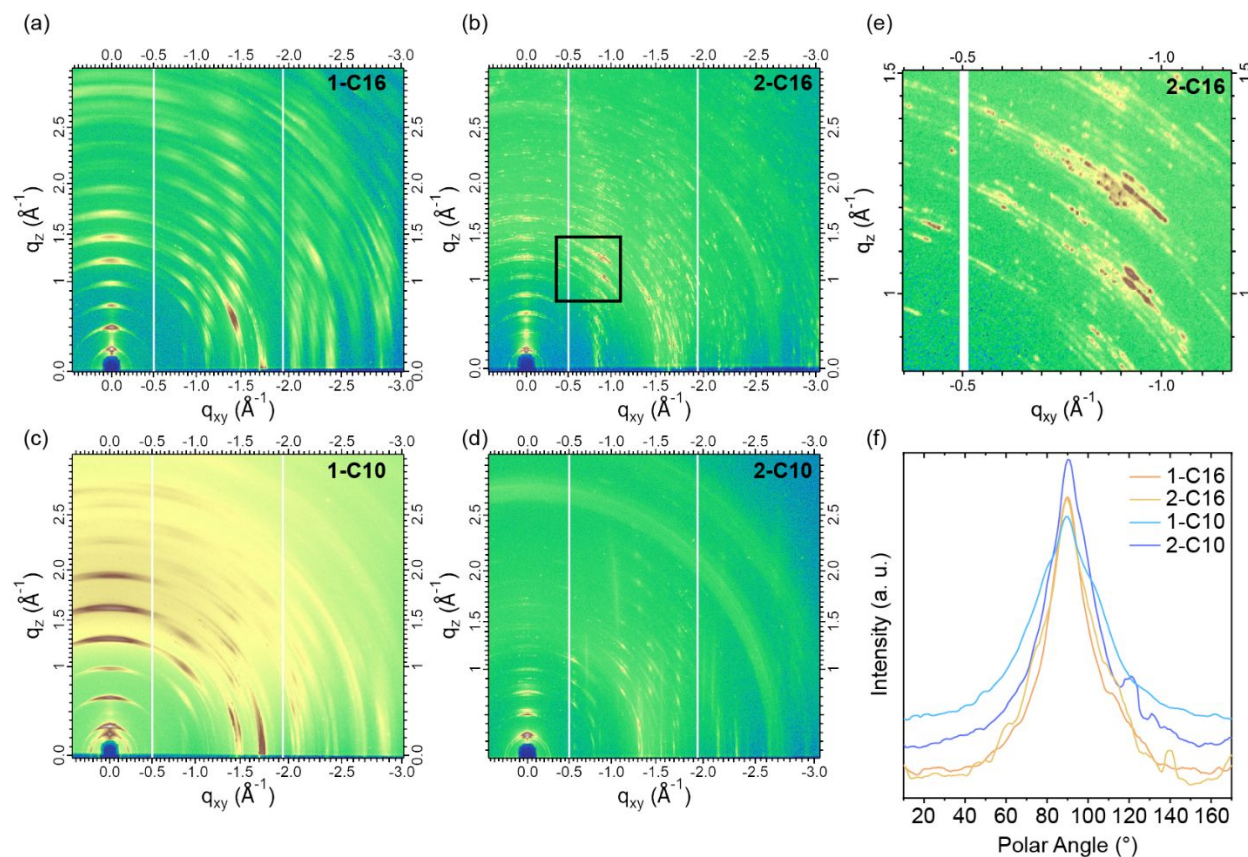


Figure 6. GIWAXS measurements of modified Ag surfaces. Two-dimensional GIWAXS images are shown for (a) 1-C16, (b) 2-C16, (c) 1-C10, and (d) 2-C10. Zoom in of the black square highlighted in (b) is shown in (e) and support that GIWAXS of 2-C16 suggest large crystallites relative to the probing area of the X-ray beam resulting in crystallites with only specific orientations being probed. The intensity vs. polar angle ($^\circ$)

for the first scattering peak, between $0.2\text{-}0.3\text{ \AA}^{-1}$, is shown for **1-C16**, **2-C16**, **1-C10**, and **2-C10** in (f) revealing crystallite orientation distribution.

This hypothesis is also supported by grazing incidence wide angle X-ray scattering (GIWAXS). With this technique, we find that, as expected, the alkyl chain number and length impacts the ordering of the alkylammonium salts in the solid state (Figure 6 and Figure S13). Quaternary ammonium salts are known to crystallize,²⁵ and the numerous defined scattering peaks present in the GIWAXS images indicates strong crystallinity.

The lowest angle scattering peaks for the four cationic modifiers at 0.25 , 0.21 , 0.32 , and 0.24 \AA^{-1} correspond to d -spacings of 2.54 , 3.02 , 1.94 , and 2.62 nm for **1-C16**, **2-C16**, **1-C10**, and **2-C10**, respectively. The **2-C16** modifier has the largest intermolecular packing distance in the solid state, and this result supports the molecular dynamics simulations that **2-C16** has a relatively more expanded structure to accommodate more CO_2 at the electrode surface. While the orientational disorder appears comparable among the different organic modifiers, **2-C16** has a propensity to form larger crystallites, as indicated by the spotted diffraction pattern (Figure 6 e-f). This results is consistent

with a much smaller contact angle of **1-C16** with respect to **2-C16** and with the RMD simulation result of **1-C16** where the hydrophilic ammonium groups are randomly distributed (Figure 3). The spacing in the nearly out-of-plane direction observed in the diffraction pattern is 2.54 nm for **1-C16** and 3.2 nm for **2-C16** (Figure 6f). This difference may be due to the larger gauche fraction in **2-C16**, as shown in the MD simulation structures.

From examining how cationic ammonium salts influence CO formation, we find that the defining parameters are both the length of the longest hydrocarbon chain and the number of these chains. The way in which these ammonium salts interact with each other is key to the observed change in selectivity, rather than how they interact with the surrounding aqueous environment.

CONCLUSION

These results lead to 97% CO formation at -0.8 V vs. RHE, with an 8-fold increase in activity relative to the bare Ag surface. With respect to our previous findings on Cu modified surfaces, the availability of CO₂ molecules at the catalytic site seems the dominant factor when CO is the only CO₂ reduction product, such as on Ag surfaces at low potential. Furthermore, we found that near optimum water availability can be achieved by controlling the ordering of the cationic modifiers. On Cu, where a proton source is needed to form both HCOOH and CO,²⁶ the hydrophilicity/phobicity of the organic modifier plays a more important role likely related to the multiple CO₂ reduction reaction products and mechanism involved.

This strategy may be useful to further improve the selectivity at low potentials and understand how the catalyst environment may be influenced by supporting organic structures in gas diffusion electrodes. More broadly, these studies provide a platform for further improvements in CO₂ reduction activity and selectivity through the design of organic species to optimize these interactions between the surrounding organic species, the aqueous environment and the catalyst surface. By selectively directing the selective

reduction of CO₂ to CO on Ag and by controlling the hydrophilicity/phobicity on Cu, future efforts in our group will focus on the fabrication of tandem catalytic systems to promote selective CO₂ conversion to specific hydrocarbons.

ASSOCIATED CONTENT

Supporting Information. Supporting Information includes supplemental experimental and theoretical procedures, data with 12 figures, and 11 tables. Raw data for histograms in Figure 2, 4, and 5 are reported in Table S2-S11.

AUTHOR INFORMATION

Corresponding Author

*fdtoste@berkeley.edu, *wag@caltech.edu, *fmtoma@lbl.gov

Author Contributions

A.K.B., F.D.T., and F.M.T. conceptualized the project. A.K.B., J.G., S.W.U carried out the experiments, and T.C. carried out the theoretical calculations. F.D.T. and F.M.T.

supervised the experimental portion and W.A.G. the theoretical portion of the project.

A.K.B., T.C., W.A.G, and F.M.T wrote the original manuscript. All authors proofread, commented on, and approved the final manuscript for submission. ‡These authors contributed equally.

Funding Sources

This material is based upon work performed by the Joint Center for Artificial Photosynthesis, a DOE Energy Innovation Hub, supported through the Office of Science of the U.S. Department of Energy under Award No. DE-SC0004993. This research used beamline 7.3.3 of the Advanced Light Source, which is a DOE Office of Science User Facility under contract no. DE-AC02-05CH11231.

ACKNOWLEDGMENT

This material is based upon work performed by the Joint Center for Artificial Photosynthesis, a DOE Energy Innovation Hub, supported through the Office of Science of the U.S. Department of Energy under Award No. DE-SC0004993.

REFERENCES

1. Gao, D.; Arán-Ais, R. M.; Jeon, H. S.; Roldan Cuenya, B., Rational Catalyst and Electrolyte Design for CO₂ Electroreduction Towards Multicarbon Products. *Nat. Catal.* **2019**, *2*(3), 198-210.
2. Waegele, M. M.; Gunathunge, C. M.; Li, J.; Li, X., How Cations Affect the Electric Double Layer and the Rates and Selectivity of Electrocatalytic Processes. *J. Chem. Phys.* **2019**, *151*(16), 160902.
3. Han, Z.; Kortlever, R.; Chen, H.-Y.; Peters, J. C.; Agapie, T., CO₂ Reduction Selective for C_{≥2} Products on Polycrystalline Copper with N-Substituted Pyridinium Additives. *ACS Cent. Sci.* **2017**, *3*(8), 853-859.
4. Li, F.; Thevenon, A.; Rosas-Hernández, A.; Wang, Z.; Li, Y.; Gabardo, C. M.; Ozden, A.; Dinh, C. T.; Li, J.; Wang, Y.; Edwards, J. P.; Xu, Y.; McCallum, C.; Tao, L.; Liang, Z.-Q.; Luo, M.; Wang, X.; Li, H.; O'Brien, C. P.; Tan, C.-S.; Nam, D.-H.; Quintero-Bermudez, R.; Zhuang, T.-T.; Li, Y. C.; Han, Z.; Britt, R. D.; Sinton, D.; Agapie, T.; Peters,

J. C.; Sargent, E. H., Molecular Tuning of CO₂-to-Ethylene Conversion. *Nature* **2020**, *577* (7791), 509-513.

5. Rosen, B. A.; Salehi-Khojin, A.; Thorson, M. R.; Zhu, W.; Whipple, D. T.; Kenis, P. J. A.; Masel, R. I., Ionic Liquid-Mediated Selective Conversion of CO₂ to CO at Low Overpotentials. *Science* **2011**, *334* (6056), 643-644.

6. Lau, G. P. S.; Schreier, M.; Vasilyev, D.; Scopelliti, R.; Grätzel, M.; Dyson, P. J., New Insights Into the Role of Imidazolium-Based Promoters for the Electroreduction of CO₂ on a Silver Electrode. *J. Am. Chem. Soc.* **2016**, *138* (25), 7820-7823.

7. García Rey, N.; Dlott, D. D., Structural Transition in an Ionic Liquid Controls CO₂ Electrochemical Reduction. *J. Phys. Chem. C* **2015**, *119* (36), 20892-20899.

8. Papisizza, M.; Cuesta, A., In Situ Monitoring Using ATR-SEIRAS of the Electrocatalytic Reduction of CO₂ on Au in an Ionic Liquid/Water Mixture. *ACS Catal.* **2018**, *8* (7), 6345-6352.

9. Ringe, S.; Clark, E. L.; Resasco, J.; Walton, A.; Seger, B.; Bell, A. T.; Chan, K., Understanding Cation Effects in Electrochemical CO₂ Reduction. *Energy Environ. Sci.* **2019**, *12*(10), 3001-3014.
10. Quan, F.; Xiong, M.; Jia, F.; Zhang, L., Efficient Electroreduction of CO₂ on Bulk Silver Electrode in Aqueous Solution via the Inhibition of Hydrogen Evolution. *Appl. Surf. Sci.* **2017**, *399*, 48-54.
11. Rosen, B. A.; Haan, J. L.; Mukherjee, P.; Braunschweig, B.; Zhu, W.; Salehi-Khojin, A.; Dlott, D. D.; Masel, R. I., In Situ Spectroscopic Examination of a Low Overpotential Pathway for Carbon Dioxide Conversion to Carbon Monoxide. *J. Phys. Chem. C* **2012**, *116*(29), 15307-15312.
12. Tanner, E. E. L.; Batchelor-McAuley, C.; Compton, R. G., Carbon Dioxide Reduction in Room-Temperature Ionic Liquids: The Effect of the Choice of Electrode Material, Cation, and Anion. *J. Phys. Chem. C* **2016**, *120*(46), 26442-26447.

13. Lim, H.-K.; Kwon, Y.; Kim, H. S.; Jeon, J.; Kim, Y.-H.; Lim, J.-A.; Kim, B.-S.; Choi, J.; Kim, H., Insight into the Microenvironments of the Metal–Ionic Liquid Interface during Electrochemical CO₂ Reduction. *ACS Catal.* **2018**, *8*(3), 2420-2427.
14. Buckley, A. K.; Lee, M.; Cheng, T.; Kazantsev, R. V.; Larson, D. M.; Goddard lii, W. A.; Toste, F. D.; Toma, F. M., Electrocatalysis at Organic–Metal Interfaces: Identification of Structure–Reactivity Relationships for CO₂ Reduction at Modified Cu Surfaces. *J. Am. Chem. Soc.* **2019**, *141*(18), 7355-7364.
15. Lobaccaro, P.; Singh, M. R.; Clark, E. L.; Kwon, Y.; Bell, A. T.; Ager, J. W., Effects of Temperature and Gas–Liquid Mass Transfer on the Operation of Small Electrochemical Cells for the Quantitative Evaluation of CO₂ Reduction Electrocatalysts. *Phys. Chem. Chem. Phys.* **2016**, *18*(38), 26777-26785.
16. Hatsukade, T.; Kuhl, K. P.; Cave, E. R.; Abram, D. N.; Jaramillo, T. F., Insights into the Electrocatalytic Reduction of CO₂ on Metallic Silver Surfaces. *Phys. Chem. Chem. Phys.* **2014**, *16*(27), 13814-13819.

17. Seifitokaldani, A.; Gabardo, C. M.; Burdyny, T.; Dinh, C.-T.; Edwards, J. P.; Kibria, M. G.; Bushuyev, O. S.; Kelley, S. O.; Sinton, D.; Sargent, E. H., Hydronium-Induced Switching between CO₂ Electroreduction Pathways. *J. Am. Chem. Soc.* **2018**, *140* (11), 3833-3837.
18. Wang, Z.; Wu, L.; Sun, K.; Chen, T.; Jiang, Z.; Cheng, T.; Goddard, W. A., Surface Ligand Promotion of Carbon Dioxide Reduction through Stabilizing Chemisorbed Reactive Intermediates. *J. Phys. Chem. Lett.* **2018**, *9* (11), 3057-3061.
19. Osman, M. A., Organo-vermiculites: synthesis, structure and properties. Platelike nanoparticles with high aspect ratio. *J. Mater. Chem.* **2006**, *16* (29), 3007-3013.
20. van Duin, A. C. T.; Bryantsev, V. S.; Diallo, M. S.; Goddard, W. A.; Rahaman, O.; Doren, D. J.; Raymond, D.; Hermansson, K., Development and Validation of a ReaxFF Reactive Force Field for Cu Cation/Water Interactions and Copper Metal/Metal Oxide/Metal Hydroxide Condensed Phases. *J. Phys. Chem. A* **2010**, *114* (35), 9507-9514.

21. Hahn, C.; Jaramillo, T. F., Using Microenvironments to Control Reactivity in CO₂ Electrocatalysis. *Joule* **2020**, *4* (2), 292-294.
22. Widom, B., Some Topics in the Theory of Fluids. *J. Chem. Phys.* **1963**, *39* (11), 2808-2812.
23. Morisato, A.; Miranda, N. R.; Freeman, B. D.; Hopfenberg, H. B.; Costa, G.; Grosso, A.; Russo, S., The influence of chain configuration and, in turn, chain packing on the sorption and transport properties of poly(tert-butyl acetylene). *J. Appl. Polym. Sci.* **1993**, *49* (12), 2065-2074.
24. Bui, J. C.; Kim, C.; Weber, A. Z.; Bell, A. T., Dynamic boundary layer simulation of pulsed CO₂ electrolysis on a copper catalyst. *ACS Energy Lett.* **2021**, *6* (4), 1181-1188.
25. Munera-Orozco, C.; Ocampo-Cardona, R.; Cedeno, D. L.; Toscano, R. A.; Rios-Vasquez, L. A., Crystal structures of three new N-halomethylated quaternary ammonium salts. *Acta Cryst. E* **2015**, *71* (10), 1230-1235.

26. Nitopi, S.; Bertheussen, E.; Scott, S. B.; Liu, X.; Engstfeld, A. K.; Horch, S.;
Seger, B.; Stephens, I. E. L.; Chan, K.; Hahn, C.; Nørskov, J. K.; Jaramillo, T. F.;
Chorkendorff, I., Progress and Perspectives of Electrochemical CO₂ Reduction on
Copper in Aqueous Electrolyte. *Chem. Rev.* **2019**, *119* (12), 7610-7672.

SYNOPSIS

